The Conjugate Electron Excitation in a Substrate – Adsorbate System

A. R. CHOLACH and V. M. TAPILIN

G. K. Boreskov Institute of Catalysis, Siberian Branch of the Russian Academy of Sciences, Pr. Akademika Lavrentyeva 5, Novosibirsk 630090 (Russia)

E-mail: cholach@catalysis.nsk.su

Abstract

The electronic peculiarities of the Pt(100)–(1 × 1) surface effected by various adsorbates and interactions in adsorbed layer were studied by the Disappearance Potential Spectroscopy (DAPS). Two types of features were observed in DAPS spectra. The first type corresponds to an ordinary threshold excitation of platinum core electron to an available vacant state. These features are attributed to the substrate properties, and their positions are in good agreement with corresponding Local Density of States (LDOS) calculations. The second type of features evidences for a new way of primary electron energy consumption – the conjugate electron excitation, which includes the above threshold transition of the substrate core electron, accompanied by excitation of the valence electron of adsorbed species to vacuum level. Positions of the respective spectral satellites are close to corresponding ionization potentials of a given species in adsorbed layer. Our experimental data show altogether more than 10 satellites, providing the evidence of reliability of the conjugate electron excitation process. The present results as a whole experimentally demonstrate the substantial unity of the substrate and adsorbate electronic structures.

INTRODUCTION

The Disappearance Potential Spectroscopy (DAPS) is known to provide information on the density of vacant states (DVS) structure of a studied sample [1–3]. The DAPS spectrum represents a current of quasielastically scattered electrons *versus* an energy of primary electrons. When the primary electron energy slightly exceeds the threshold energy, an incident electron can transmit its energy to the core electron, so that both electrons move to states just above the Fermi level (E_F). The DAPS spectral features are mainly determined by self-convolution of density of states above E_F [1–3]. Using DAPS, one can find additional information on the chemical bond origin and on the DVS in the surface region. However, DAPS is not widely used by now, and there is insufficient number of papers dealing with this technique. The DAPS loses in comparison with the Auger Electron Spectroscopy (AES), X-ray Photoelectron Spectroscopy (XPS), Ultraviolet Photoelectron Spectroscopy (UPS), *etc.* as a surface analysis method. At the same time, the sensitivity of DAPS spectral features to the nature of surrounding surface species and to the presence of impurities or adsorbed residual gases makes this technique very promising for studying adsorption and catalysis.

We have previously shown [4–6] that DAPS can be successfully used for the examination of platinum electronic properties. The DAPS spectra are in agreement with the Local Density of States (LDOS) calculations and with the known model of hydrogen adsorption on the unreconstructed Pt(100) single crystal surface. The present paper is aimed at studying the effect of chemisorption on the electronic peculiarities of platinum surface.

THEORY

We present here the calculations of bulk platinum DOS that have been performed with the ADF-BAND (Amsterdam Density Functional) code [7]. This code uses the density func-

tional formalism, numerical atomic and Slater functions as a basis set, and numerical integration over the real space for calculations of the Hamiltonian matrix elements, that permitted to avoid muffin-tin approximation for the crystal potential. We used the local density approximation with Vosko – Wilk – Nusair formulas for exchange-correlation potential [8] and the spin-restricted nonrelativistic option of the program. Numerical atomic functions from 1*s* up to 6*s*, calculated with Herman – Skillman program [9], and 5*d*, 6*s* and 6*p* Slater functions were used as the basis functions. The integration over the Brillouin zone was performed with the quadratic interpolations of band structure.

Figure 1, *A* presents the results of DOS calculations for the bulk platinum in the vicinity and above the E_F. For assignment of the DAPS peaks, the important features are: a relatively small part of *d*-electron states above the E_F, and the DOS peaks near 10 and 15 eV. The corresponding energy regions are shaded and denoted as *a*, *b* and *d*. The region *c* between *a* and *b* states corresponds to the broad peak of DOS. According to the self-convolution model of Lander [10], working quite well for a number of solids, the line shape in DAPS is determined by the following equation:

$$\frac{dW}{dE} = \frac{d}{dE}\int_0^E \rho(\varepsilon)\rho(E-\varepsilon)d\varepsilon = \rho(0)\rho(E) + \int_0^E \rho(\varepsilon)\frac{d\rho(E-\varepsilon)}{dE}d\varepsilon \quad (1)$$

where ρ and *W* are the Pt bulk DOS and DOS self-convolution, respectively.

The result of calculation using this equation for DOS, shown in Fig. 1, *A*, is presented in Fig. 1, *B*. One can expect the following features in DAPS spectra: just above the E_F (peak *a*), at 10 and 15 eV above the E_F (peaks *b* and *d*) and a broad feature *c* between peaks *a* and *b*. All the mentioned features, except *d*, are in the agreement with our earlier calculations based on the LMTO-TB approximation [5].

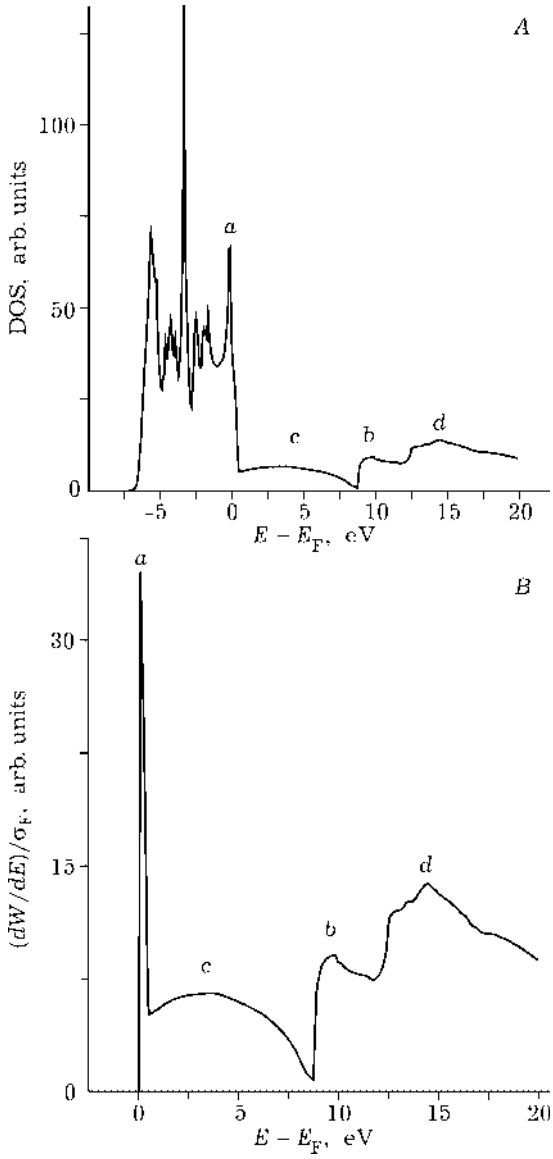

Fig. 1. Pt bulk DOS (density of states = the number of states per energy unit per atom); *a*, *b*, *c*, and *d* are the DOS features revealed in DAPS spectra (see Fig. 2) (*A*), and derivative of the Pt bulk DOS self-convolution *W* normalized by state density at the Fermi level σ_F (*B*). The features *a*, *b*, *c* and *d* correspond to those in DOS.

EXPERIMENTAL

Experiments were performed in an UHV chamber with a residual gas pressure of $<1\ 10^{-10}$ mbar, which was equipped with the instrumentation for Low-Energy Electron Diffraction (LEED) and AES, a dipole mass spectrometer and an Ar^+ ion gun. The DAPS technique was arranged by the use of 3-grid LEED optics. The central LEED electron gun with a tungsten cathode was used as a source of primary electrons of variable energy. The surface cleanliness was checked by AES. The finally observed LEED pattern was typical for the Pt(100)-*hex* surface [11, 12]. The clean unreconstructed Pt(100)–(1 × 1) surface was obtained using "NO-receipt" from [13, 14].

The detailed description of experimental technique and sample treatment can be found elsewhere [4]. The apparent Pt $4d_{5/2}$ core level energy of (314.8 ± 0.5) eV (*i. e.* E_F location) was determined as an intersection of background and leading edge of the spectral peak [2, 4], and it is close to the reference value of 314.6 eV [15].

Since DAPS deals with an elastic electron collection, it certainly accumulates the attendant diffraction features, which are up to 10^3 times larger than those of true DAPS peaks, that is why the latter are completely masked. This is particularly pronounced for the well-ordered substrate, such as single crystal surface. In Fig. 2, *A*, the survey DAPS spectra exhibit a continuous sequence of such peaks with mean width at the base of about 15–20 eV, which is a typical characteristic of diffraction features [16]. In order to separate the strong diffraction background, we followed the difference between DAPS spectra of clean and adsorbate-covered surfaces. Thus, the diffraction features suppress each other in difference spectrum under subtraction. The difference DAPS spectrum (S_{dif}) was computed from the recorded spectra of clean (S_{cl}) and adsorbate-covered (S_{ads}) surfaces according to the equation:

$$S_{dif} = \alpha(\theta) S_{ads} - S_{cl} \qquad (2)$$

where $\alpha(\theta)$ accounts for the screening effect of the adsorbed layer at coverage θ, corresponding to the given exposure; this procedure we described earlier in more detail [4].

The sequential construction of difference spectrum is demonstrated in Fig. 2, *B*. In the present work we studied the Pt(100)–(1 × 1) surface in order to maintain the stable substrate structure, because the Pt(100)-*hex* surface is known to reconstruct readily under the influence of various adsorbates [17, 18]. The threshold excitation of Pt 4*f* core electrons is expected to be more effective in comparison with that of 4*d* electrons [19]. Nevertheless, we have investigated an energy range of 300–350 eV around the Pt 4*d* core level. Figure 2, *A* shows that this energy range is more convenient due to a smaller diffraction peak intensity, compared to the energy range of 70–80 eV around the Pt 4*f* binding energy.

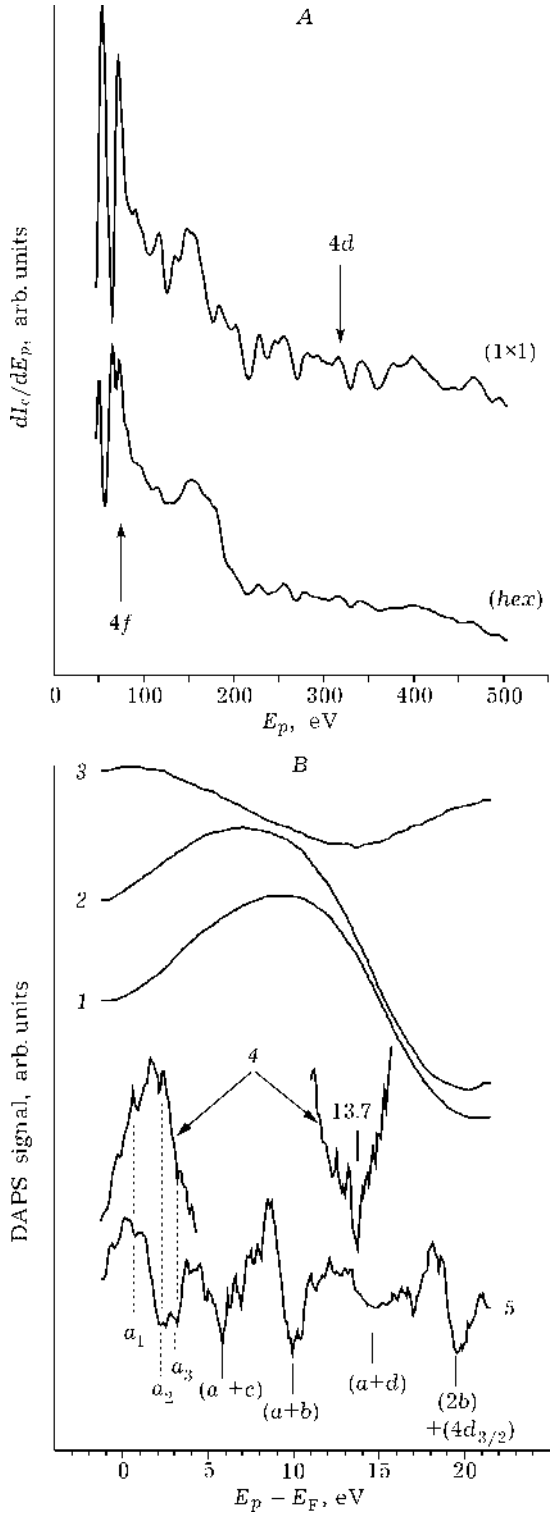

Fig. 2. Survey DAPS spectra of the clean Pt(100) surface with (1×1) and *hex* structures of the top layer (*A*), and DAPS spectra after hydrogen adsorption on the Pt(100)–(1×1) surface (*B*): *1* and *2* – original DAPS spectra corresponding to the clean surface and after H_2 exposure of 6 L (Langmuir), respectively; *3* and *4* – difference DAPS spectra, *4* is identical to *3*, but magnified 25 times; *5* – difference DAPS spectrum corresponding to H_2 exposure of 0.9 L, *4* and *5* are displayed at the same ordinate scale.

RESULTS AND DISCUSSION

Figures 2 and 3 present a set of difference DAPS spectra, corresponding to various adsorbed layers on the clean Pt(100)−(1 × 1) surface. The vacant states in DAPS spectra shown in these figures and in the text are labeled in accordance with LDOS features in Fig. 1.

Figure 2, *B* shows the spectra obtained after two different H_2 exposures. A considerable difference between these spectra results from the ordering in H_{ads} layer at higher hydrogen exposure. Indeed, the low- and high-energy parts in spectrum *4* correspond to the top and bottom of the total spectrum *3*, respectively, whereas spectrum *5* does not show the attending diffraction feature. Spectra *4* and *5* reveal a triply splitted *a*-state, corresponding to the DOS structure of Pt 5*d* band [4−6]. The other spectral features are labeled in accordance with the location of two interacting electrons (incident and excited) for different DOS peaks shown in Fig. 1 [4]. The peak at 19−20 eV above Pt $4d_{5/2}$ threshold is most probably contributed by the sum of double occupation of *b*-state and the threshold excitation of $4d_{3/2}$ core level [4]. Besides the splitted *a*-state, the high-energy region in spectrum *4* reveals a pronounced peak at 13.7 eV, whose origin will be discussed below.

Figure 3, *A* shows DAPS spectra obtained after various CO exposures. The strong diffraction background, resulting from the ordered adsorbed layer formation, significantly hampers the expected fine spectral structure just above the E_F. However, two unresolved peaks at ~12.6 and 13.8 eV are quite pronounced. As CO exposure rises, the intensities of both peaks are increasing, and the intensity ratio changes in favor of the latter peak. In addition, the feature at ~18.3 eV is also seen. To assign the peaks, their positions were compared to the reference data on the respective ionization potentials of CO_{ads} (Table 1). It should be noted

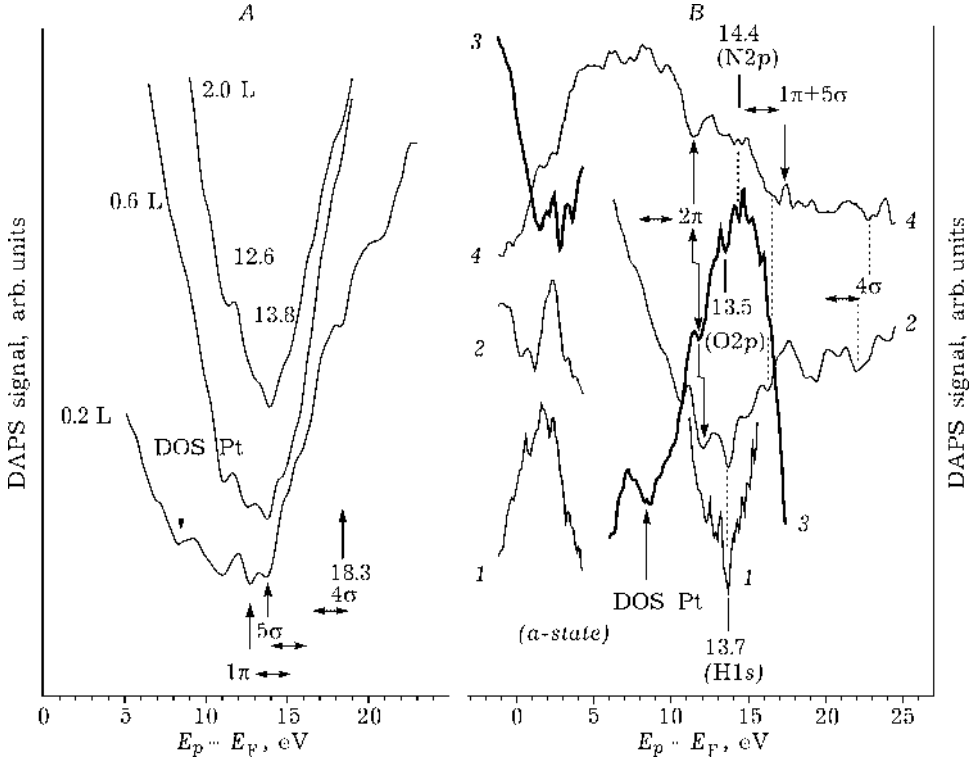

Fig. 3. Difference DAPS spectra related to CO adsorption on clean Pt(100)−(1 × 1) surface at 300 K and shown exposures (in Langmuirs) (*A*), and comparative set of difference DAPS spectra related to interaction of NO with hydrogen-covered Pt(100)−(1 × 1) surface (*B*): *1* − after 6 L H_2 exposure on clean surface; *2* − after exposure of surface *1* to 0.7 L of NO; *3* − after further exposure of surface *2* to NO up to total NO exposure of 1.0 L (this curve is displayed in bold type in order to distinguish it from other spectra at intersection points); *4* − after exposure of clean Pt(100)-*hex* surface to 20 L of NO at 300 K; the double-side arrows correspond to width and locations of the respective valence states obtained from the reference UPS data.

TABLE 1

Comparison of high-energy DAPS feature positions (the peak minimum above E_F, eV) revealed after CO adsorption on Pt(100)−(1×1) surface as shown in Fig. 3, *A* with ionization potentials (eV) estimated for the similar systems

Inquiry object	DAPS features			Ref.
	1π	5σ	4σ	
CO_{gas}	14.01	16.53	19.68	[15, 28]
CO/Pt(100)-*hex*	14.6 (1π + 5σ)		17.2	[28]
CO/Pt(111)	14.2	15.05	17.45	[28, 29, 31]
CO/Pt foil	14.6 (1π + 5σ)		17.1	[30]
CO/Pt(100)−(1×1)				
0.2 L	12.7	13.7	18.3	This work
0.6 L	12.6	13.8	~18.3 (masked)	
2.0 L	12.6	13.9	~18.3 (masked)	

Note. Ionization potentials are determined as a sum of UPS peak positions with respect to E_F and the corresponding work function.

that different platinum surfaces reveal similar features in the UPS spectra obtained after O_2, NO, and CO adsorption [20−26]. Unfortunately, the values of corresponding work functions required for the determination of ionization potentials are not available. In Fig. 3, *A*, the spectral feature at ~20.9 eV likely belongs to platinum DOS function [4].

Figure 3, *B* shows the DAPS spectra obtained after separate adsorption of H_2 and NO, and in the course of interaction NO_{gas} + H_{ads}. There is also a set of additional features, which can not be treated as a combination of platinum LDOS peculiarities. Even a brief revision of data presented in Table 2 shows the correspondence between positions of DAPS peaks

TABLE 2

Comparison of high-energy DAPS feature positions (the peak minimum above E_F, eV) revealed after H_2 and NO adsorption and NO_{gas} + H_{ads} interaction on Pt(100)−(1×1) surface as shown in Fig. 3, *B* with ionization potentials (eV) estimated for the similar adsorbed species

Inquiry object	DAPS features							Ref.
	H 1*s*	O 2*p*	N 2*p*	NO				
				2π	1π	5σ	4σ	
$H_{2,gas}$ + NO_{gas}	13.60	13.62	14.54	9.3	16.9	17.4	21.0	[15, 31]
O/Pt(100)	–	12.7	–	–	–	–	–	[28]
O/Pt(111)	–	14.2	–	–	–	–	–	[32]
O/Pt(111)	–	12.1	–	–	–	–	–	[29, 33]
H/Pt(111)	12.8	–	–	–	–	–	–	[33]
NO/Pt(100)-*hex*	–	12.1 (O 2*p* + N 2*p*)		8.9	15.7 (1π + 5σ)		20.7	[21, 28]
NO/Pt(100)-*hex*	–	–	–	8.4	15.5 (1π + 5σ)		20.2	[17]
NO/Pt(111)	–	–	–	7.9	14.9	18.0	20.7	[31]
6 L H_2/Pt(100)−(1×1)	13.7	–	–	–	–	–	–	This work
0.7 L NO_{gas} + H_{ads}	13.7 (H 1*s* + O 2*p*)		–	12.0	16.3 (1π + 5σ)		22.2	
1.0 L NO_{gas} + H_{ads}	–	13.5	14.4	11.8	15.9 (1π + 5σ)		22.5[a]	
20 L NO/Pt(100)-*hex*	–	13.8 (O 2*p* + N 2*p*)		11.4	15.9		23	

Note. Ionization potentials are determined as a sum of UPS peak positions with respect to E_F and the corresponding work function.

[a]Peak is not shown in Fig. 3, *B*; its position is estimated after subtraction of the linear background.

and respective values of the valence band ionization potentials. Indeed, if the hydrogen-covered surface (spectrum *1*) is exposed to 0.7 Langmuirs (L) of NO, the H 1*s* peak at 13.7 eV depletes, a new strong peak appears at 12.0 eV and weak features appear at 16.3 and 22.2 eV. A decrease of the former peak intensity corresponds to a removal of H_{ads} from the surface due to NO_{ads} dissociation [21, 27], followed by reaction $2H_{ads} + O_{ads} \rightarrow H_2O_{gas}$. It should be noted that spectrum *2* in Fig. 3, *B* was obtained under the same experimental conditions as in [27], where authors have shown the formation of stable $NH_{2,\,ads}$ species. We suppose that in the present case formation of the same species attributes the pronounced feature at 12.0 eV, whose position is close to ionization potential of the $NH_{2,\,gas}$ species, which is 11.14 eV [15]. The peak at 12.0 eV slightly shifts and diminishes upon further NO exposure (spectrum *3*), which corresponds to the removal of $NH_{2,\,ads}$ species under these experimental conditions [27]. The positions of new pronounced peak at 14.4 eV and weak features at 15.9 and 22.5 eV in spectrum *3* are also close to the respective ionization potentials of N_{ads} and NO_{ads} species (see Table 2). The presence of molecularly adsorbed NO_{ads} on platinum surface is quite possible in our experimental conditions [17], and atomic N_{ads} species may form due to the NO_{ads} dissociation and/or the primary electron beam damage of NO_{ads} [20]. Because of the last reason, the peak at 13.5 eV in spectrum *3* should be related not to H_{ads}, but to O_{ads} species, as noted in Table 2. The additional strong feature at 8.5 eV in spectrum *3* is probably associated with the excitation of Pt 5*d* electrons, since it is localized within the characteristic energy region of strong UPS peaks corresponding to the different platinum surfaces [15, 17, 28]. Peak positions revealed after 20 L exposure of the clean Pt(100)-*hex* surface to NO (spectrum *4*) are close to the corresponding ionization potentials, which were determined under similar experimental conditions (see Table 2).

According to the data listed in Tables 1 and 2, DAPS spectra generally reveal high-energy satellites, which can not be described according to our earlier approach as a combination of platinum vacant states occupied by operating electrons [4–6]. Moreover, positions of these satellites with respect to the substrate E_F are close to ionization potentials of the species in adsorbed layer. This evidences for a new way of primary electron energy relaxation, which includes the excitation of substrate core level, accompanied by the threshold ionization of atoms and/or molecules forming the adsorbed layer. The simultaneous energy transfer, followed by localization of the primary and core electrons in the vacant *a*-state just above E_F, may be realized as follows:

$$e_p^- + 4d_0^{10} + V^2 + a^0 \rightarrow 4d_{5/2}^9 + V^1 + a^2 + e_{em}^- \qquad (3)$$

where e_p^- is a primary electron, e_{em}^- is electron emitted from the given valence state *V*.

Then the energy conservation condition should be written according to the below equation:

$$E_p = E_B + I + 2\varepsilon_a \qquad (4)$$

where E_p, E_B and I stand for absolute values of the primary electron energy, core level binding energy, and ionization potential of valence state *V*, respectively; ε_a stands for the energy of vacant *a*-state above E_F.

On the one hand, the position of DAPS satellite must exceed the respective ionization potential by $2\varepsilon_a$, according to eq. (4). On the other hand, the satellite position must be lower than the ionization potential determined from UPS data. This is due to the derivative mode of experimental DAPS spectra, because position of the DAPS peak minimum should correspond to the leading edge of broad UPS feature. However, the agreement between DAPS and UPS data (see Tables 1 and 2) seems to be significant, though one can not expect a precise conformity. It is very unlikely that the above DAPS satellites are originated from the spectra subtraction technique and/or imperfection of the surface structure, because of the significant difference between widths of satellite and diffraction peaks [16]. Our experimental data show altogether more than 10 satellites, providing the evidence of reliability of the conjugate electron excitation process [4].

The core and valence electrons separately are an ordinary objects for the admission of external energy. The DAPS technique is actually a probe, which reveals energy thresholds of the primary electron current consumption.

Our data indicate that a threshold conjugate excitation of both core and valence electrons becomes possible if E_p in eq. (4) overpowers the sum of E_B and I. This process should not be considered as an excitation of core electron of a Pt atom directly to the atomic orbital of adsorbed atom. Instead, we suggest that ionization of the adsorbed species results from excitation of the metal core electron to the metal valence orbital, which is strongly associated through a chemical bond with an orbital of adsorbed species. Moreover, the intensities of such features in DAPS spectra may be considered as a measure of chemical bond strength. The presence of similar features at 8–9 eV above E_F in DAPS spectra related to the clean and adsorbate-covered surface (see Fig. 3, *B* and [4]) indicates, that valence state V in eq. (3) may belong to the substrate and to the adsorbed species as well. Moreover, based on the detailed analysis of DAPS spectra, we assume that the platinum plasmons characterized by a neighbor energy difference of (6.0 ± 0.8) eV are distinguishable [4].

The DAPS spectral satellites corresponding to conjugate electron excitation are in qualitative accordance with the electronic peculiarities of solids, revealed by the other techniques. Indeed, these features are similar to those of the shake-off satellites in AES and XPS spectra [29, 30]. They correspond to the relaxation of core hole, accompanied by the emission of valence electron of the *same atom* into continuum. On the other hand, the UPS technique evidences that the substrate and adsorbate electronic properties are quite specific. Besides, emission of *both the substrate and adsorbate* valence electrons is readily exhibited in UPS spectra. The DAPS principle differs significantly from that of AES, XPS and UPS. It concerns the incident particles, the excitation mechanism, the conformational interaction, the final state structure, *etc.* However, all these techniques deal with the similar electronic peculiarities, which should be of the same origin. In summary, our data show that excitation of the *substrate* core electron, accompanied by the excitation of valence electron of the *neighboring adsorbed species*, seems to be very probable. Moreover, this emphasizes a strong correlation between the substrate and adsorbate electronic structures.

CONCLUSIONS

1. The electronic peculiarity of the Pt(100)–(1×1) surface affected by different adsorbates was studied by the Disappearance Potential Spectroscopy (DAPS). The two types of features were revealed in DAPS spectra:

(i) The first type of features corresponds to the ordinary threshold excitation of the platinum core electron to available vacant state. These features are mainly attributed to the substrate properties, and faintly depend on the adsorbate nature. The peak positions are in a good agreement with Local Density of States (LDOS) calculations related to platinum unoccupied states;

(ii) The second type of features evidences for the conjugate electron transition, which includes the above excitation of the substrate core electron, and excitation of the valence electron of adsorbed species to vacuum level. The positions of respective satellites in the DAPS spectra strongly depend on the adsorbate nature.

2. The present experimental results demonstrate the substantial unity of the substrate and adsorbate electronic structure, and display capabilities of the DAPS technique to reveal peculiarities of the surface unoccupied states and valence states, corresponding to both the substrate and adsorbate.

Acknowledgement

The authors appreciate the financial support from INTAS Grant 99–01882.

REFERENCES

1 J. Kirschner, in H. Ibach (Ed.), Electron Spectroscopy for Surface Analysis, Springer-Verlag, 1977, Ch. 3.
2 R. L. Park, *Surf. Sci.*, 48 (1975) 80.
3 L. Ecertová, *Ibid.*, 200 (1988) 490.
4 A. R. Cholach, V. M. Tapilin, *Appl. Surf. Sci.*, 180 (2001) 173; *J. Mol. Catal.*, 158 (2000) 181; A. R. Cholach, V. M. Tapilin, in L. Petrov, Ch. Bonev, G. Kadinov (Eds.), Heterogeneous Catalysis, Proc. 9th Intern. Symp. on Heterog. Catal., Varna, Bulgaria, 23–27 Sept., 2000, Sofia, 2000, p. 73.

5 A. R. Cholach, V. M. Tapilin, Abstr. Intern. Memorial K. I. Zamaraev Conf. "Physical Methods for Catalytic Research at the Molecular Level", Novosibirsk, Russia, 1999, p. 56.
6 A. R. Cholach, V. M. Tapilin, *React. Kinet. Catal. Lett.*, 71 (2000) 65.
7 G. de Velde and E. J. Baerends, *Phys. Rev. B*, 44 (1991) 7888.
8 S. H. Vosko, L. Wilk and M. Nusair, *Canadian J. Phys.*, 58 (1980) 1200.
9 F. Herman and S. Skillman, in: Atomic Structure Calculations, Prentice-Hill, Inc., 1963.
10 J. Lander, *Phys. Rev.*, 91 (1953) 1382.
11 Ch. Romainczyk, J. R. Manson, K. Kern *et al., Surf. Sci.*, 336 (1995) 362.
12 A. T. Pasteur, St. J. Dixon-Warren, D. A. King, *J. Chem. Phys.*, 103 (1995) 2251.
13 G. Brodén, G. Briden, H. P. Bonzel, *Surf. Sci.*, 72 (1978) 45.
14 D. Yu. Zemlyanov, M. Yu. Smirnov, V. V. Gorodetskii, *Catal. Lett.*, 43 (1997) 181.
15 Handbook of Chemistry and Physics, 73rd ed., in D. R. Lide (Ed.), CRC Press, Inc., 1992–1993, pp. 10–281.
16 D. P. Woodruff, in D. A. King and D. P. Woodruff (Eds.), The Chemical Physics of Solid Surfaces and Heterogeneous Catalysis, vol. 1: Clean Solid Surfaces, Elsevier Sci. Publ. Co., 1981, ch. 2, pp. 81–181.
17 H. P. Bonzel, G. Brodén, G. Pirug, *J. Catal.*, 53 (1978) 96.
18 H. Miki, T. Nagase, K. Sato *et al.*, *Surf. Sci.*, 287/288 (1993) 448.
19 Practical Surface Analysis by Auger and X-ray Photoelectron Spectroscopy, in D. Briggs and M. P. Seach (Eds.), John Wiley&Sons, 1983; T. A. Carlson, Photoelectron and Auger Spectroscopy, Plenum Press, 1975, ch. 4, 5; D. P. Woodruff, T. A. Delchar, Modern Techniques of Surface Science, Cambridge Univ. Press, 1986, ch. 3.
20 D. M. Collins, W. E. Spicer, *Surf. Sci.*, 69 (1977) 114.
21 S. Sugai, K. Takeuchi, T. Ban *et al., Ibid.*, 282 (1993) 67.
22 S. R. Bare, K. Griffiths, P. Hofmann *et al., Ibid.*, 120 (1982) 367.
23 J. L. Gland, B. E. Sexton, G. B. Fisher, *Ibid.*, 95 (1980) 587.
24 S. Sugai, K. Shimizu, H. Watanabe *et al., Ibid.*, 287/288 (1993) 455.
25 H. Miki, T. Kioka, S. Sugai, K. Kawasaki, *Vacuum*, 41 (1990) 105.
26 J. Küppers, G. Ertl, *Surf. Sci. Lett.*, 77 (1978) L647.
27 D. Yu. Zemlyanov, M. Yu. Smirnov, V. V. Gorodetskii, *Ibid.*, 391 (1997) 37.
28 H. P. Bonzel, T. E. Fischer, *Ibid.*, 51 (1975) 213.
29 A. Ramstad, F. Strisland, S. Raaen *et al., Ibid.*, 440 (1999) 290.
30 A. I. Boronin, P. A. Zhdan, *Izv. AN SSSR. Ser. fiz.*, 46 (1982) 1247, and private communication.
31 M. E. Bartram, B. E. Koel, E. A. Carter, *Surf. Sci.*, 219 (1989) 467.
32 C. Puglia, A. Nilsson, B. Hernnäs *et al., Ibid.*, 342 (1995) 119.
33 J. E. Demuth, *Ibid.*, 65 (1977) 369.